UNIVERSIDAD DE CONCEPCIÓN

Centro de Investigación en Ingeniería Matemática (CI^{2}MA)

An hp finite element adaptive method to compute the vibration modes of a fluid-solid coupled system

Maria G. Armentano, Claudio Padra,
Rodolfo Rodríguez, Mario Scheble

PREPRINT 2010-05

SERIE DE PRE-PUBLICACIONES

An *hp* finite element adaptive method to compute the vibration modes of a fluid-solid coupled system

M. G. Armentano [1], C. Padra [2], R. Rodríguez [3] and M. Scheble [2,*]

[1] *Departamento de Matemática, Facultad de Ciencias Exactas y Naturales, Universidad de Buenos Aires, 1428, Buenos Aires, Argentina*
[2] *Centro Atómico Bariloche, 4800, Bariloche, Argentina*
[3] *CI²MA, Departamento de Ingeniería Matemática, Universidad de Concepción, Casilla 160-C, Concepción, Chile*

SUMMARY

In this paper we propose an *hp* finite element method to solve a two-dimensional fluid-structure vibration problem. This problem arises from the computation of the vibration modes of a bundle of parallel tubes immersed in an incompressible fluid. We use a residual-type a posteriori error indicator to guide an *hp* adaptive algorithm. Since the tubes are allowed to be different, the weak formulation is a non-standard generalized eigenvalue problem. This feature is inherited by the algebraic system obtained by the discretization process. We introduce an algebraic technique to solve this particular spectral problem. We report several numerical tests which allow us to assess the performance of the scheme.

KEY WORDS: fluid structure interaction, vibration problem, *hp* finite element adaptive method

1. INTRODUCTION

In this work we consider an *hp* finite element adaptive scheme for solving a fluid-structure interaction problem, which corresponds to computing the vibrations of a bundle of parallel tubes immersed in a fluid contained in a rigid cavity.

The numerical solution of spectral problems arising in fluid mechanics have been receiving increasing attention (see [1, 5, 6, 9, 10, 16] and the references therein). In particular, the problem considered in this paper has a considerable importance in nuclear engineering and has been studied for several authors (see, for example, [9, 17, 18]). The method of added mass (see, for example, [9, 10]) consists in transforming this model into a second order ODE system for the displacement vectors. However, in this process, it is necessary to solve a finite number of source problems which makes difficult to design an adaptive algorithm, since the singularities of each of these problems do not match, in general, with the singularities of the vibration modes.

*Correspondence to: scheble@cab.cnea.gov.ar

It is well known that adaptive procedures based on a posteriori error indicators play nowadays a relevant role in the numerical solution of partial differential equations and, in particular, in eigenvalue problems. There are several papers for the classical h version of finite element methods concerning the development of efficient adaptive schemes for different eigenvalue problems (see, for example, [2, 11, 12, 13, 14]) and there are also some recent references regarding the hp finite element solution of eigenvalue problems (see, for instance, [4, 7, 8]). However, the bibliography about hp-adaptive schemes for this kind of problems is scarce. One of the main difficulties in hp-adaptivity arises from the fact that the accuracy can be improved in two different ways, either by subdividing elements or by increasing the polynomial degree.

In a recent paper [3], we have introduced and analyzed an hp finite element solver of the spectral problem described above. We have proposed an adaptive scheme and applied it to different cavities and shapes of tubes. However, in all the examples considered in that article, the tubes have been assumed to be identical, with the same mass and stiffness. The reason for this is that when the tubes are not all identical, the resulting spectral problem is not any longer a standard generalized eigenvalue problem and it is not clear at all how it could be efficiently solved.

In this paper we propose an strategy to solve this particular algebraic spectral problem. It consists in transforming it into an equivalent standard generalized eigenvalue problem which can be solved with classical eigensolvers. Moreover, such an strategy allows us to extend the results from [3] to derive an hp finite element adaptive method which can be applied to bundles of tubes with different shapes, rigidities and masses. Therefore, we are able to perform a much more complete numerical experimentation, which allows us to assess the performance of the proposed adaptive scheme.

The rest of the paper is organized as follows. In Section 2 we recall the fluid-solid vibration problem and introduce the hp finite element method, the a posteriori error estimator and the adaptive refinement strategy. In Section 3 we propose an algorithm to solve the algebraic spectral problem. The algorithm can be efficiently combined with the refinement scheme in such a way that it performs the adaptive process by considering the actual singularities of the vibration modes. In Section 4 we report different numerical examples which allow assessing the performance of the adaptive scheme. Finally, we end the paper drawing some conclusions in Section 5.

2. THE SPECTRAL PROBLEM AND THE *hp* FINITE ELEMENT ADAPTIVE SCHEME

We consider a coupled system composed of K elastically mounted parallel tubes immersed in a fluid inside a rigid cavity. The problem is to determine the free vibration modes of the system.

Under reasonable assumptions (see [10]), this problem can be posed in a two-dimensional (2D) framework, a planar transverse section of the cavity being its domain. Tube number i is modeled as a harmonic oscillator with stiffness k_i and mass m_i, whereas the fluid is taken as perfectly incompressible with density ρ.

We call Ω the bounded 2D domain occupied by the fluid, Γ_0 its outer boundary and Γ_i the interfaces between each tube and the fluid. (See Figure 1.)

The problem of computing the vibration modes of the coupled system consists in finding the free vibration frequencies ω and the corresponding amplitudes of the fluid pressure variation

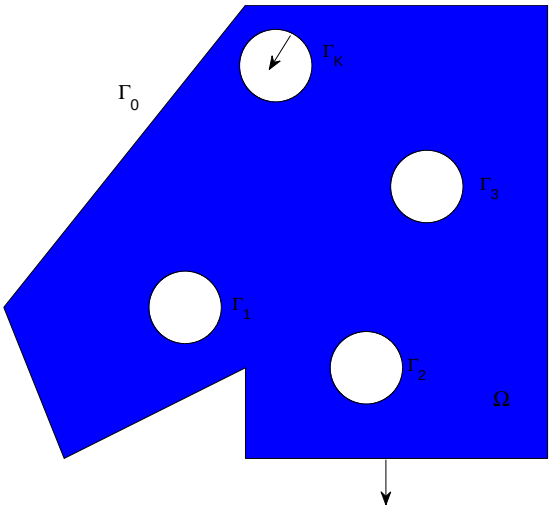

Figure 1. Sketch of the 2D domain

u, which satisfy

$$\begin{cases} \Delta u = 0 & \text{in } \Omega, \\ \dfrac{\partial u}{\partial n} = 0 & \text{on } \Gamma_0, \\ \dfrac{\partial u}{\partial n} = \dfrac{\rho\omega^2}{k_i - m_i\omega^2} \left(\displaystyle\int_{\Gamma_i} u\boldsymbol{n} \right) \cdot \boldsymbol{n} & \text{on } \Gamma_i, \quad i = 1, \ldots, K, \end{cases} \tag{2.1}$$

where $\boldsymbol{n}$ denotes the unit outer normal to the boundary of Ω.

Let $\mathscr{V} := \left\{ v : \Omega \to \mathbb{R} : \int_\Omega \left(|v|^2 + |\nabla v|^2 \right) < \infty \right\}$ (i.e., $\mathscr{V}$ is the Sobolev space $H^1(\Omega)$). The variational form of problem (2.1) reads as follows: Find $\omega > 0$ and a non-vanishing $u \in \mathscr{V}$ such that

$$\int_\Omega \nabla u \cdot \nabla v = \sum_{i=1}^{K} \frac{\rho\omega^2}{k_i - m_i\omega^2} \left(\int_{\Gamma_i} u\boldsymbol{n} \right) \cdot \left(\int_{\Gamma_i} v\boldsymbol{n} \right) \qquad \forall v \in \mathscr{V}. \tag{2.2}$$

We note that (2.2) is not a standard generalized eigenvalue problem, because there is not a unique eigenvalue multiplying a bilinear form on the right-hand side, but different rational functions of ω multiplying different bilinear forms for each tube. The existence of the solution to this problem has been analyzed in [10, Section II.2.1]. It was proved in this reference that this non-standard eigenvalue problem attains $2K$ vibration frequencies with corresponding linearly independent eigenfunctions (recall that K is the number of tubes).

2.1. The hp finite element method

We introduce an *hp* finite element method to compute the solution of problem (2.2). Let $\mathscr{T}_h$ be a triangular mesh in Ω such that any two triangles share at most a vertex or an edge. Let

h stand for the mesh-size; namely, $h := \max_{T\in\mathscr{T}_h} h_T$, with h_T being the length of the largest edge of the triangle T. We assume that $\mathscr{T}_h$ satisfies a minimum angle condition.

We associate with each element $T \in \mathscr{T}_h$ a (maximal) polynomial degree $p_T \in \mathbb{N}$. We assume that the polynomial degrees of neighboring elements are comparable, i.e., there exists a constant $\gamma > 0$ such that

$$\gamma^{-1} p_T \le p_{T'} \le \gamma p_T \qquad \forall T,\, T' \in \mathscr{T}_h \text{ with } T \cap T' \neq \emptyset. \tag{2.3}$$

We call $\boldsymbol{p} := \{p_T\}_{T\in\mathscr{T}_h}$ the family of polynomial degrees for each triangle.

Throughout the paper, we will denote by C a generic positive constant, not necessarily the same at each occurrence, which may depend on the mesh and the degree of the polynomials only through the minimal angle and the parameter γ, respectively.

We define the finite element space as follows:

$$\mathscr{V}_h^{\boldsymbol{p}} := \{v : \Omega \to \mathbb{R} \text{ continuous} :\ v|_T \in \mathscr{P}_{p_T}\ \forall T \in \mathscr{T}_h\} \subset \mathscr{V},$$

where $\mathscr{P}_{p_T}$ denotes the set polynomials of degree at most p_T. Notice that the definition of $\mathscr{V}_h^{\boldsymbol{p}}$ allows for different polynomial degrees on each edge of any triangle. Therefore, the space $\{v|_T :\ v \in \mathscr{V}_h^{\boldsymbol{p}}\}$ does not necessarily contain all the polynomials of degree p_T. However, there exists $p'_T \le p_T$ such that

$$\mathscr{P}_{p'_T} \subset \{v|_T :\ v \in \mathscr{V}_h^{\boldsymbol{p}}\} \subset \mathscr{P}_{p_T} \tag{2.4}$$

and $p_T/p'_T \le \gamma$ because of assumption (2.3).

The discrete eigenvalue problem associated with (2.2) is the following: Find ω_h and a non-vanishing $u_h \in \mathscr{V}_h^p$ such that

$$\int_\Omega \nabla u_h \cdot \nabla v_h = \sum_{i=1}^{K} \frac{\rho\omega_h^2}{k_i - m_i\omega_h^2} \left(\int_{\Gamma_i} u_h \boldsymbol{n}\right) \cdot \left(\int_{\Gamma_i} v_h \boldsymbol{n}\right) \qquad \forall v_h \in \mathscr{V}_h^{\boldsymbol{p}}. \tag{2.5}$$

This is a non-standard algebraic eigenvalue problem too, for the same reasons as above. The theory in [10, Section II.2.1] holds also in this case and allows proving that this discrete problem attains $2K$ vibration frequencies with corresponding linearly independent eigenfunctions. In principle it is not clear how such a non-linear problem could be efficiently solved. However, we will show in Section 3 that it can be reduced to an equivalent well-posed generalized matrix eigenvalue problem, which can be solved with standard techniques.

We have obtained in [3] the following a priori error estimates for the computed vibration frequencies ω_h and the associated eigenfunctions u_h (which correspond to the fluid pressure), in the case that all the tubes have the same mass and stiffness.

Theorem 2.1. *There holds*

$$|\omega - \omega_h| \le C \left(\frac{h}{p}\right)^{2r} \qquad \textit{and} \qquad \int_\Omega |\nabla u - \nabla u_h|^2 \le C \left(\frac{h}{p}\right)^{2r},$$

where $r < \frac{\pi}{\theta}$, with θ being the largest reentrant angle of Ω.

2.2. A posteriori error estimates

In what follows we introduce an a posteriori indicator for the error in the energy norm of the pressure.

For each inner edge ℓ, we choose a unit normal vector $\boldsymbol{n}_\ell$ and denote the two triangles sharing this edge T_{in} and T_{out}, with $\boldsymbol{n}_\ell$ pointing outwards T_{in}. We set

$$\left[\!\left[\frac{\partial u_h}{\partial n} \right]\!\right]_\ell := \nabla \left(u_h|_{T_{\text{out}}} \right) \cdot \boldsymbol{n}_\ell - \nabla \left(u_h|_{T_{\text{in}}} \right) \cdot \boldsymbol{n}_\ell,$$

which corresponds to the jump of the normal derivative of u_h across the edge ℓ. Notice that this value is independent of the chosen direction of the normal vector $\boldsymbol{n}_\ell$.

Let us define, for each edge ℓ,

$$J_\ell := \begin{cases} \dfrac{1}{2} \left[\!\left[\dfrac{\partial u_h}{\partial n} \right]\!\right]_\ell, & \text{if } \ell \text{ is an inner edge,} \\ \dfrac{\partial u_h}{\partial n}, & \text{if } \ell \subset \Gamma_0, \\ \dfrac{\partial u_h}{\partial n} - \left(\displaystyle\int_{\Gamma_i} \lambda_i u_h \boldsymbol{n} \right) \cdot \boldsymbol{n}, & \text{if } \ell \subset \Gamma_i, \quad i = 1, \ldots, K. \end{cases}$$

For each element $T \in \mathscr{T}_h$, we define the local error indicator η_T by

$$\eta_T^2 := \frac{h_T^2}{p_T^2} \left\| \Delta u_h \right\|_{L^2(T)}^2 + \sum_{\ell \text{ edge of } T} \frac{|\ell|}{p_\ell} \left\| J_\ell \right\|_{L^2(\ell)}^2, \tag{2.6}$$

with $p_\ell := \max \{ p_T : T \supset \ell \}$, and the global error estimator η_Ω by

$$\eta_\Omega^2 := \sum_{T \in \mathscr{T}_h} \eta_T^2.$$

We have obtained in [3] the following a posteriori error estimates in case that all the tubes have the same mass and stiffness.

Theorem 2.2. *i) There exists a positive constant C such that*

$$\int_\Omega |\nabla(u - u_h)|^2 \leq C \left[\eta_\Omega^2 + \left(\frac{h}{p} \right)^{4r} \int_\Omega |\nabla(u - u_h)|^2 \right].$$

ii) For all $\delta > 0$, there exists a positive constant C_δ such that for all $T \in \mathscr{T}_h$, if T has only inner edges or edges on Γ_0, then

$$\eta_T^2 \leq C_\delta p_T^{2+\delta} \int_{\omega_T} |\nabla(u - u_h)|^2$$

and, if T has an edge lying on Γ_i, $i = 1, \ldots, K$, then

$$\eta_T^2 \leq C_\delta p_T^{2+\delta} \left[\int_{\omega_T} |\nabla(u - u_h)|^2 + \frac{h_T^2}{p_T^2} \left| \int_{\Gamma_i} (\lambda u - \lambda_h u_h) \boldsymbol{n} \right|^2 \right],$$

where $\omega_T := \bigcup \{ T' : \ T \text{ and } T' \text{ share an edge} \}$.

This theorem yields the reliability of the error estimator η_Ω (up to higher order terms) and the efficiency of the error indicator η_T.

2.3. Adaptive refinement strategy

There are several strategies to determine which elements should be refined in an h-finite element adaptive scheme. A usual one is the so-called *maximum strategy* in which all the triangles T with $\eta_T \geq \theta\eta_{\mathrm{M}}$ are marked to be refined, where

$$\eta_{\mathrm{M}}^2 := \frac{1}{\#\mathscr{T}_h} \sum_{T\in\mathscr{T}_h} \eta_T^2$$

and $\theta > 0$ is a parameter which can be arbitrarily chosen.

Our *hp* adaptive algorithm uses this strategy to mark the triangles to be refined, with the additional consideration that, at each step, for each marked triangle, it has to be decided whether to perform a p-refinement or an h-refinement. In the case of p-refinement, the degree p_T of the marked element is increased by one and the triangle is kept fixed. On the other hand, in the case of h-refinement, the marked element T is subdivided into four triangles, $T = \bigcup_{j=1}^4 T_j'$, and the degree is kept fixed in the new elements, i.e., $p_{T_j'} = p_T$. Moreover, the conformity of the mesh is preserved by means of a longest edge subdivision strategy on the unrefined neighboring triangles (see [19]). Because of this, it happens that some elements not marked for h-refinement, are subdivided anyway into two or three triangles. Thus, in general, we will have that $T = \bigcup_{j=1}^k T_j'$ with $k = 2$, 3 or 4.

In order to decide whether to apply a p or an h refinement to a particular triangle, we follow the approach proposed in [15], which is based on the comparison of the current local estimated error with a prediction of this error obtained from the preceding step. If at the preceding step there was an h refinement leading to $T = \bigcup_{j=1}^k T_j'$, $k = 2, 3, 4$, then the prediction indicator is defined as follows:

$$\left(\eta_{T_j'}^{\mathrm{pred}}\right)^2 := \gamma_h \left(\frac{|T_j|}{|T|}\right)^{p_T+1} \eta_T^2,$$

where γ_h is a control parameter to be determined. On the other hand, if at the preceding step there was a p refinement on the element T, then the prediction indicator is defined by

$$\left(\eta_T^{\mathrm{pred}}\right)^2 := \gamma_p \eta_T^2,$$

where $\gamma_p \in (0, 1)$ is a reduction factor which is chosen arbitrarily. Finally, for elements neither p nor h refined at the preceding step,

$$\left(\eta_T^{\mathrm{pred}}\right)^2 := \gamma_n \left(\eta_T^{\mathrm{pred}}\right)^2,$$

where γ_n is another parameter also arbitrarily chosen. In all cases, we proceed to an h refinement of T when the error indicator η_T is larger than the prediction indicator η_T^{pred} and to a p refinement otherwise.

Altogether, we arrive at the algorithm shown in Table I.

We set $\eta_T^{\mathrm{pred}} := 0$ for all elements T on the initial triangulation, so that the first step is a purely h-refinement on all elements. Notice that this ensures that no triangle will have vertices lying on two different Γ_i on subsequent meshes (this will be useful for the procedure that we will propose to solve the generalized eigenvalue problem).

Table I. Refinement algorithm

```
If η_T^2 ≥ θ η_M^2 then
    if η_T^2 ≥ (η_T^pred)^2 then
        subdivide T into 4 triangles T'_j, 1 ≤ j ≤ 4
        longest edge strategy to maintain mesh conformity
        p_{T_j} := p_T
        (η_{T_j}^pred)^2 := γ_h ( |T_j| / |T| )^{p_T+1} η_T^2
    else
        p_T := p_T + 1
        (η_T^pred)^2 := γ_p η_T^2
    end
else
    (η_T^pred)^2 := γ_n (η_T^pred)^2
end
```

3. SOLUTION OF THE NON STANDARD MATRIX EIGENVALUE PROBLEM

In this section we analyze some numerical aspects concerning the solution of the non-standard eigenvalue problem (2.5).

First notice that the solutions of both, the continuous problem (2.2) and the discrete one (2.5), are determined up to an additive constant. In fact, it is simple to check that if u is a solution of (2.2), then $u + c$ is also a solution of the same problem for any constant c and the same vibration frequency ω. Exactly the same happens with problem (2.5).

To fix uniquely a solution of problem (2.5), it is enough to set its value to zero at a given node of the mesh. With this end, we choose an arbitrary fixed node $P_0 \in \Gamma_0$ (the same for all meshes in the adaptive process) and restrict the finite element space to the functions in $\mathscr{V}_h^{\boldsymbol{p}}$ which vanish at that node P_0.

We denote by $\mathscr{N}$ the set of nodes of the finite element space excluding P_0 and decompose it as follows: $\mathscr{N} = \mathscr{N}_1 \cup \mathscr{N}_2$, with $\mathscr{N}_1 = \bigcup_{i=1}^{K} \mathscr{N}^{(i)}$, where $\mathscr{N}^{(i)}$ is the subset of nodes lying on Γ_i, $1 \le i \le K$, and $\mathscr{N}_2$ is the subset of the remaining ones (i.e., the nodes lying either in Ω or on Γ_0).

We denote by M_i the number of nodes of $\mathscr{N}^{(i)}$ $(i = 1, \ldots, K)$ and by N_i the number of nodes on $\mathscr{N}_i$ $(i = 1, 2)$. Notice that $N_1 = M_1 + \cdots + M_K$ is the total number of nodes lying on all the interfaces Γ_i, whereas N_2 is the number of the remaining nodes minus one (P_0). Consequently, for a fine mesh, N_1 has to be significantly smaller than N_2.

Let

$$\boldsymbol{u}_1 := \big(u(P_i)\big)_{P_i \in \mathscr{N}_1} \in \mathbb{R}^{N_1} \qquad \text{and} \qquad \boldsymbol{u}_2 := \big(u(P_i)\big)_{P_i \in \mathscr{N}_2} \in \mathbb{R}^{N_2}.$$

The matrix form of the discrete problem (2.5) reads as follows:

$$\begin{pmatrix} \boldsymbol{A}_{11} & \boldsymbol{A}_{12} \\ \boldsymbol{A}_{21} & \boldsymbol{A}_{22} \end{pmatrix} \begin{pmatrix} \boldsymbol{u}_1 \\ \boldsymbol{u}_2 \end{pmatrix} = \begin{pmatrix} \boldsymbol{\Lambda}\boldsymbol{B}_{11} & \boldsymbol{0} \\ \boldsymbol{0} & \boldsymbol{0} \end{pmatrix} \begin{pmatrix} \boldsymbol{u}_1 \\ \boldsymbol{u}_2 \end{pmatrix}, \tag{3.1}$$

where

$$\boldsymbol{A}_{rs} := \left(\int_\Omega \nabla\beta_i \cdot \nabla\beta_j \right)_{P_i\in\mathscr{N}_r, P_j\in\mathscr{N}_s}, \quad r,s = 1,2,$$

with $\{\beta_i\}_{P_i\in\mathscr{N}}$ being the nodal basis (i.e., $\beta_i(P_j) = \delta_{ij}$), $\boldsymbol{\Lambda}$ is a diagonal matrix given by

$$\boldsymbol{\Lambda} := \begin{pmatrix} \lambda_1 \boldsymbol{I}_{M_1\times M_1} & & \\ & \ddots & \\ & & \lambda_K \boldsymbol{I}_{M_K\times M_K} \end{pmatrix}, \qquad \text{with } \lambda_i := \frac{\rho\omega_h^2}{k_i - m_i\omega_h^2}, \quad i = 1,\dots,K,$$

($\boldsymbol{I}_{M_i\times M_i}$ denotes the $M_i \times M_i$ identity matrix), and

$$\boldsymbol{B}_{11} := \begin{pmatrix} \boldsymbol{B}^{(1)} & & \\ & \ddots & \\ & & \boldsymbol{B}^{(K)} \end{pmatrix},$$

with $\boldsymbol{B}^{(l)} \in \mathbb{R}^{M_l\times M_l}$ defined by

$$\boldsymbol{B}^{(l)} := \left(\left(\int_{\Gamma_i} \beta_i \boldsymbol{n} \right) \cdot \left(\int_{\Gamma_i} \beta_j \boldsymbol{n} \right) \right)_{P_i,P_j\in\mathscr{N}^{(l)}}, \qquad l = 1,\cdots,K.$$

Our goal is to transform (3.1) into a standard symmetric generalized eigenvalue problem of size $2K$ (which is know to be the number of solutions of this problem). We observe that the matrix on the left hand side of (3.1) is symmetric and positive definite, while the one on the right hand side is symmetric and positive semi-definite. Then, since the submatrix $\boldsymbol{A}_{22}$ is invertible (indeed, symmetric and positive definite), by eliminating $\boldsymbol{u}_2$ from (3.1) we arrive at

$$\boldsymbol{C}\boldsymbol{u}_1 = \boldsymbol{\Lambda}\boldsymbol{B}_{11}\boldsymbol{u}_1, \tag{3.2}$$

with $\boldsymbol{C} = \boldsymbol{A}_{11} - \boldsymbol{A}_{12}\boldsymbol{A}_{22}^{-1}\boldsymbol{A}_{21}$.

This problem is equivalent to (3.1). Notice that although the matrix $\boldsymbol{C}$ is not sparse, its dimension is N_1 and, hence, as stated above, significantly smaller than the size $N_1 + N_2$ of problem (3.1). Moreover, in actual computations, the matrix $\boldsymbol{A}_{22}^{-1}$ is not explicitly computed. In fact, the columns of $\boldsymbol{A}_{22}^{-1}\boldsymbol{A}_{12}$ are obtained by solving N_1 linear systems with the same matrix $\boldsymbol{A}_{22} \in \mathbb{R}^{N_2\times N_2}$, which is sparse, symmetric and positive definite.

As a second step, we compute a complete diagonalization of the matrix $\boldsymbol{B}_{11}$. As far as the mesh have no triangles with vertices lying on two different Γ_i, this matrix is block diagonal with K full diagonal blocks, the dimension of each one being M_i. Thus, any standard eigensolver for symmetric matrices (QR, for instance) can be conveniently used for each diagonal block and provide us with orthogonal matrices $\boldsymbol{Q}^{(i)}$, $1 \le i \le K$, such that

$$\boldsymbol{Q}^{(i)^{\mathrm{t}}}\boldsymbol{B}^{(i)}\boldsymbol{Q}^{(i)} = \boldsymbol{D}^{(i)} := \operatorname{diag}\left\{\mu_1^{(i)}, \mu_2^{(i)}, 0, \dots, 0\right\},$$

with $\mu_1^{(i)} \neq 0$ and $\mu_2^{(i)} \neq 0$.

Thus, if we define

$$\boldsymbol{Q} := \begin{pmatrix} \boldsymbol{Q}^{(1)} & & \\ & \ddots & \\ & & \boldsymbol{Q}^{(K)} \end{pmatrix},$$

we have that

$$\boldsymbol{Q}^{\mathrm{t}}\boldsymbol{B}_{11}\boldsymbol{Q} = \boldsymbol{D},$$

with

$$\boldsymbol{D} = \begin{pmatrix} \boldsymbol{D}^{(K)} & & \\ & \ddots & \\ & & \boldsymbol{D}^{(K)} \end{pmatrix}.$$

Let $\boldsymbol{v} := \boldsymbol{Q}^{\mathrm{t}}\boldsymbol{u}_1$ and $\boldsymbol{S} := \boldsymbol{Q}^{\mathrm{t}}\boldsymbol{C}\boldsymbol{Q}$, since $\boldsymbol{Q}^{\mathrm{t}}\boldsymbol{\Lambda}\boldsymbol{Q} = \boldsymbol{\Lambda}$ (because the columns of $\boldsymbol{Q}$ are orthogonal), problem (3.2) is equivalent to the following one:

$$\boldsymbol{S}\boldsymbol{v} = \boldsymbol{\Lambda}\boldsymbol{D}\boldsymbol{v}. \tag{3.3}$$

Matrix $\boldsymbol{D}$ is diagonal with only $2K$ non-zero diagonal entries: $\mu_1^{(1)}, \mu_2^{(1)}, \ldots, \mu_1^{(K)}, \mu_2^{(K)}$. Let $\boldsymbol{P}$ be a permutation matrix such that

$$\tilde{\boldsymbol{D}} := \boldsymbol{P}^{\mathrm{t}}\boldsymbol{D}\boldsymbol{P} := \begin{pmatrix} \tilde{\boldsymbol{D}}_{11} & \boldsymbol{0} \\ \boldsymbol{0} & \boldsymbol{0} \end{pmatrix}, \qquad \text{with} \qquad \tilde{\boldsymbol{D}}_{11} := \operatorname{diag}\left\{\mu_1^{(1)}, \mu_2^{(1)}, \ldots, \mu_1^{(K)}, \mu_2^{(K)}\right\}.$$

Then, (3.3) is equivalent to

$$\tilde{\boldsymbol{S}}\tilde{\boldsymbol{v}} = \tilde{\boldsymbol{\Lambda}}\tilde{\boldsymbol{D}}\tilde{\boldsymbol{v}}, \tag{3.4}$$

where $\tilde{\boldsymbol{S}} := \boldsymbol{P}^{\mathrm{t}}\boldsymbol{S}\boldsymbol{P}$, $\tilde{\boldsymbol{v}} := \boldsymbol{P}^{\mathrm{t}}\boldsymbol{v}$, $\tilde{\boldsymbol{\Lambda}} := \boldsymbol{P}^{\mathrm{t}}\boldsymbol{\Lambda}\boldsymbol{P}$ and $\tilde{\boldsymbol{D}}$ is as defined above.

Since $\boldsymbol{\Lambda}$ is diagonal, $\tilde{\boldsymbol{\Lambda}}$ is diagonal too and it can be decomposed in blocks as follows:

$$\tilde{\boldsymbol{\Lambda}} = \begin{pmatrix} \tilde{\boldsymbol{\Lambda}}_{11} & \boldsymbol{0} \\ \boldsymbol{0} & \tilde{\boldsymbol{\Lambda}}_{22} \end{pmatrix}, \qquad \text{with} \qquad \tilde{\boldsymbol{\Lambda}}_{11} := \operatorname{diag}\left\{\lambda_1, \lambda_1, \ldots, \lambda_K, \lambda_K\right\}.$$

This leads to the following block decomposition of (3.4):

$$\begin{pmatrix} \tilde{\boldsymbol{S}}_{11} & \tilde{\boldsymbol{S}}_{12} \\ \tilde{\boldsymbol{S}}_{21} & \tilde{\boldsymbol{S}}_{22} \end{pmatrix} \begin{pmatrix} \tilde{\boldsymbol{v}}_1 \\ \tilde{\boldsymbol{v}}_2 \end{pmatrix} = \begin{pmatrix} \tilde{\boldsymbol{\Lambda}}_{11} & \boldsymbol{0} \\ \boldsymbol{0} & \tilde{\boldsymbol{\Lambda}}_{22} \end{pmatrix} \begin{pmatrix} \tilde{\boldsymbol{D}}_{11} & \boldsymbol{0} \\ \boldsymbol{0} & \boldsymbol{0} \end{pmatrix} \begin{pmatrix} \tilde{\boldsymbol{v}}_1 \\ \tilde{\boldsymbol{v}}_2 \end{pmatrix} = \begin{pmatrix} \tilde{\boldsymbol{\Lambda}}_{11}\tilde{\boldsymbol{D}}_{11} & \boldsymbol{0} \\ \boldsymbol{0} & \boldsymbol{0} \end{pmatrix} \begin{pmatrix} \tilde{\boldsymbol{v}}_1 \\ \tilde{\boldsymbol{v}}_2 \end{pmatrix}.$$

Now, by eliminating $\tilde{\boldsymbol{v}}_2$ we arrive at

$$\left(\tilde{\boldsymbol{S}}_{11} - \tilde{\boldsymbol{S}}_{12}\tilde{\boldsymbol{S}}_{22}^{-1}\tilde{\boldsymbol{S}}_{21}\right)\tilde{\boldsymbol{v}}_1 = \tilde{\boldsymbol{\Lambda}}_{11}\tilde{\boldsymbol{D}}_{11}\tilde{\boldsymbol{v}}_1. \tag{3.5}$$

Let $\boldsymbol{T} := \tilde{\boldsymbol{S}}_{11} - \tilde{\boldsymbol{S}}_{12}\tilde{\boldsymbol{S}}_{22}^{-1}\tilde{\boldsymbol{S}}_{21}$ (notice that $\boldsymbol{T}$ is a symmetric matrix). Since $\tilde{\boldsymbol{\Lambda}}_{11}^{-1} = \frac{1}{\rho\omega^2}\boldsymbol{K} - \frac{1}{\rho}\boldsymbol{M}$, with

$$\boldsymbol{K} = \operatorname{diag}\left\{k_1, k_1, \ldots, k_K, k_K\right\} \qquad \text{and} \qquad \boldsymbol{M} = \operatorname{diag}\left\{m_1, m_1, \ldots, m_K, m_K\right\},$$

an easy calculation shows that problem (3.5) is equivalent to the following one:

$$\boldsymbol{K}\boldsymbol{T}\tilde{\boldsymbol{v}}_1 = \omega^2\left(\rho\tilde{\boldsymbol{D}}_{11} + \boldsymbol{M}\boldsymbol{T}\right)\tilde{\boldsymbol{v}}_1. \tag{3.6}$$

Finally, defining $\boldsymbol{w} := \boldsymbol{T}\tilde{\boldsymbol{v}}_1$, we can rewrite (3.6) as follows:

$$\tilde{\boldsymbol{D}}_{11}^{-1}\boldsymbol{K}\boldsymbol{w} = \omega^2\left(\rho\boldsymbol{T}^{-1} + \tilde{\boldsymbol{D}}_{11}^{-1}\boldsymbol{M}\right)\boldsymbol{w},$$

which is a generalized eigenvalue problem of size $2K$, with both matrices symmetric and positive definite (moreover, the matrix in the left hand side is diagonal). Thus, this is a well posed (and very small) problem that can be efficiently solved by any standard eigensolver.

4. NUMERICAL EXPERIMENTS

We present in this section some numerical results which allow us to assess the performance of the proposed *hp* adaptive refinement strategy.

The color palette, used in the figures, indicates the polynomial degree of each element.

4.1. Test 1: L-shaped cavity with different shape tubes

In this first test we have considered two octagonal tubes and a quadrilateral one within an L-shaped cavity. The position of the tubes and the initial mesh, with quadratic finite elements in all triangles, is shown in Figure 2. The fluid density ρ is set to one, whereas the physical parameters m_i and k_i are the same for all tubes and also equal to one. The second vibration mode is selected to perform the adaptive process.

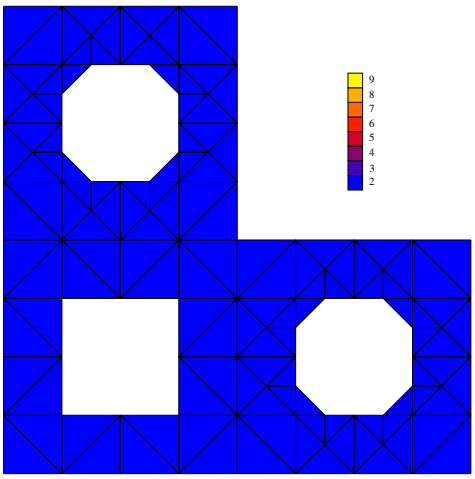

Figure 2. Test 1. Domain and initial mesh for the L-shaped cavity with different shape tubes.

In this numerical example the control parameters appearing in the algorithm, have been chosen as follows: $\theta = 0.5$, $\gamma_h = 20$, $\gamma_p = 0.4$ and $\gamma_n = 2.5$. In this case, the fluid domain has reentrant angles at the vertices of the tubes, and at the reentrant vertex of the external boundary, producing singularities which compete against each other in the refinement process.

Figure 3 shows the meshes obtained with the adaptive *hp* algorithm corresponding to the step 12 and 24 of the refinement procedure.

The behavior of the adaptive algorithm in the neighborhood of the different singularities appearing in this example can be appreciated from Figures 4 to 6. In Figure 4 we present a sequence of zooms of the mesh at step 24 around one the reentrant angles of the bottom octagon and in Figure 5 around the top right corner of the square. Figure 6 shows a sequence of zooms in the reentrant vertex of the rigid cavity. Each zoom enlarges 10 times the previous one.

In all cases we observe the typical *hp* adaptive behavior: as we approach the singularity, the order p of the elements gradually decreases, until the lowest order 2 is reached in the nearest

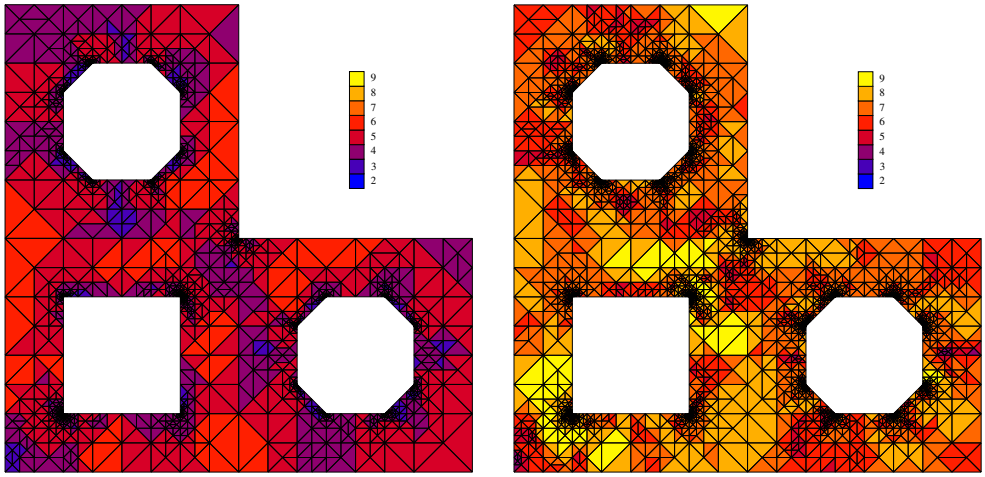

Figure 3. Test 1. Refined meshes: step 12 (left) and 24 (right)

elements to the vertex. We observe that the number of zooms required to display smaller elements, indicates that, roughly speaking, the h-refinement is similar at the vertex of the octagon and at the reentrant vertex in the external boundary, but approximately ten times less refined than near the vertex of the square, which is the dominant singularity.

Figure 7 shows the pressure field obtained at the last step and the fluid velocity field computed from this pressure. The arrows at the center of each tube show the tubes velocities.

It is known that a proper combination of h and p refinement allows to obtaining an exponential rate of convergence

$$\int_\Omega |\nabla u - \nabla u_h|^2 \leq C e^{-2\alpha\sqrt{N}},$$

where N is the number of degrees of freedom. Figure 8 exhibits a plot of $\log(\eta_\Omega)$ versus $\sqrt{N}$, which shows that the estimated error η_Ω attains such an exponential rate in this problem.

No analytical solution is available in this case to check if the actual error also attains an exponential rate of convergence. To provide some numerical evidence of such a behavior, we have estimated the error of the computed eigenvalues by using as 'exact' a more accurate computation obtained by an extrapolation procedure. To do this, we have used the fact that the computed eigenvalues are expected to converge with a double order and we have determined the parameters λ, κ and α in the model

$$\lambda_h = \lambda + \kappa \mathrm{e}^{-2\alpha\sqrt{N}},$$

by means of a weighted least-squares fitting. The weights have been chosen so that the most precise computed values λ_h play the more significant role in the fitting. Thus, we have obtained a value $\lambda = 0.136286733767$, which we have used to plot $\log|\lambda_h - \lambda|$ versus $N^{1/2}$. This plot is shown in Figure 9, where a linear dependence can be clearly seen for sufficiently large values of N. This is coherent with the expected exponential decay of the error with respect to the number of degrees of freedom.

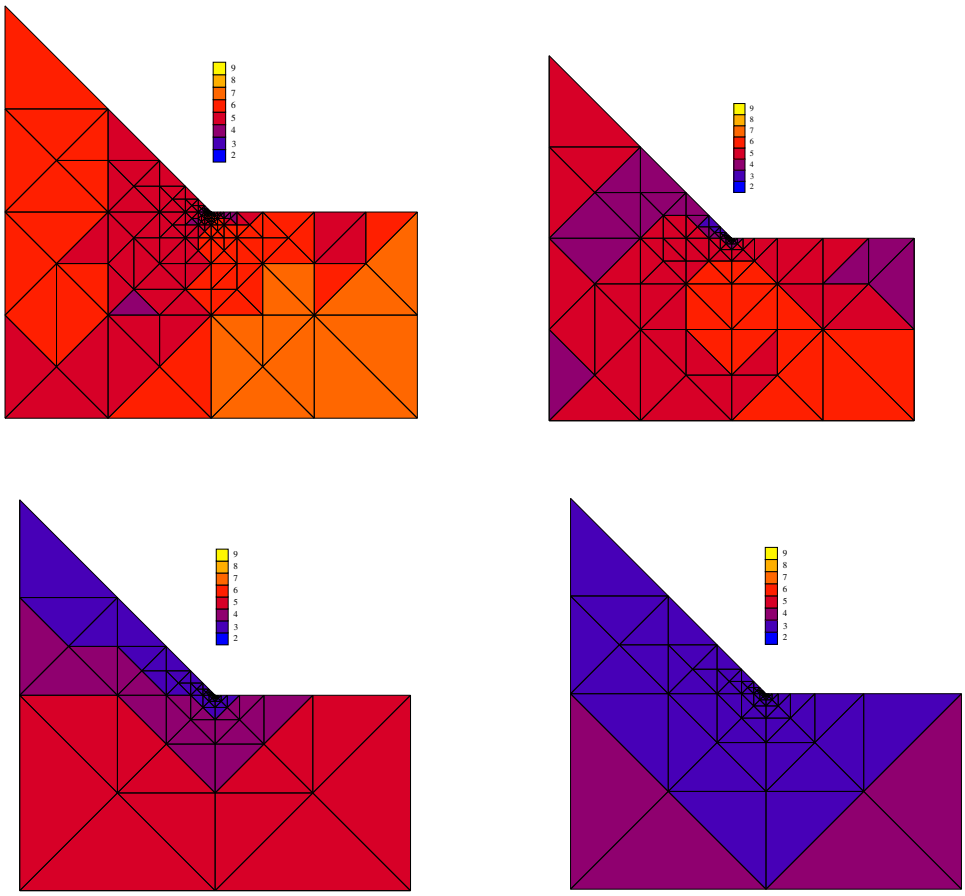

Figure 4. Test 1. Angle at a corner of an octagon tube. Refined mesh: step 24. Successive zooms

4.2. Test 2: Bundle of circular tubes with different physical parameters within a quadrilateral cavity

In this second test we have computed all the vibration modes of a system closer to the actual applications: four circular tubes with different physical parameters immersed in a fluid occupying a quadrilateral cavity. The position of the tubes and the initial mesh, with quadratic finite element in all triangles, is shown in Figure 10.

In this case, the fluid density has been taken $\rho = 1$ and the physical parameters of the tubes as follows: mass $m_i = 1$, $i = 1, \ldots, 4$ and stiffness $k_1 = k_4 = 1.05$ and $k_2 = k_3 = 1$. The control parameters appearing in the algorithm, have been chosen as follows: $\theta = 0.75$, $\gamma_h = 8$, $\gamma_p = 0.2$ and $\gamma_n = 1$.

We report in Table II the eight frequencies obtained after 8 steps of refinement.

The succession of meshes obtained during the adaptive process not only depends on the

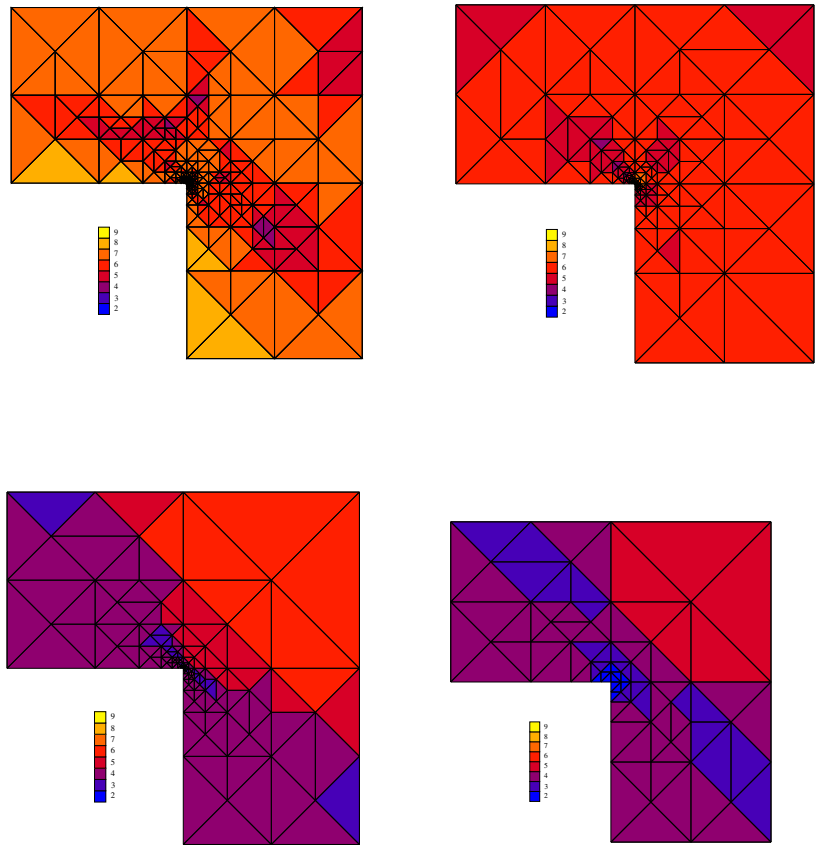

Figure 5. Test 1. Angle at a corner of the square tube. Refined mesh: step 24. Successive zooms

geometry, but also on the physical parameters of the tubes. This is obvious from the fact that different rigidities and masses can significantly change the motion of tubes, and therefore, the type of singularities present at their boundaries.

Figure 11 shows the meshes obtained after 8 steps of the *hp*-adaptive scheme for a couple of vibration modes.

Figure 12 shows the pressure fields computed with the final mesh of the adaptive process for the same vibrations modes. Figure 13 shows the corresponding fluid velocity fields. The arrows at the center of each tube show the velocities of the tubes motion. For the sake of clarity different scales have been used for representing tubes velocities and the fluid velocity field.

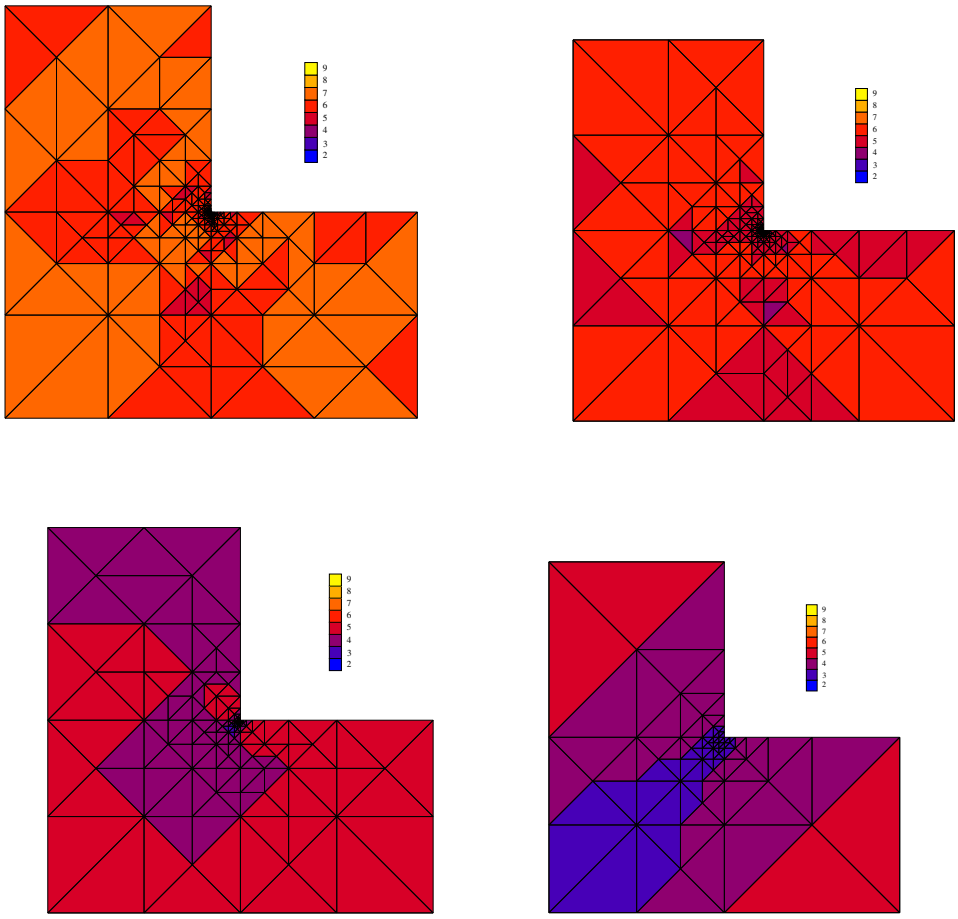

Figure 6. Test 1. Reentrant angle of the L-shaped cavity. Refined mesh: step 24. Successive zooms

5. CONCLUSIONS

An *hp* finite element method has been proposed to compute the free vibrations of a bundle of different tubes immersed in an incompressible fluid contained in a rigid cavity. This leads to a non-standard eigenvalue problem, when the tubes are not all identical.

We have introduced an algebraic procedure to transform the resulting eigenvalue problem into a small-size standard one, which can be solved with classical eigensolvers.

We have proposed an a-posteriori error indicator and an adaptive algorithm based on this indicator, which allows refining some of the elements and increasing the polynomial degree in others at each step.

The reported numerical experiments for different cavities and different shape, mass and stiffness of tubes show the good performance of the error indicator and the adaptive scheme. The succession of meshes obtained during the adaptive process not only depends on the

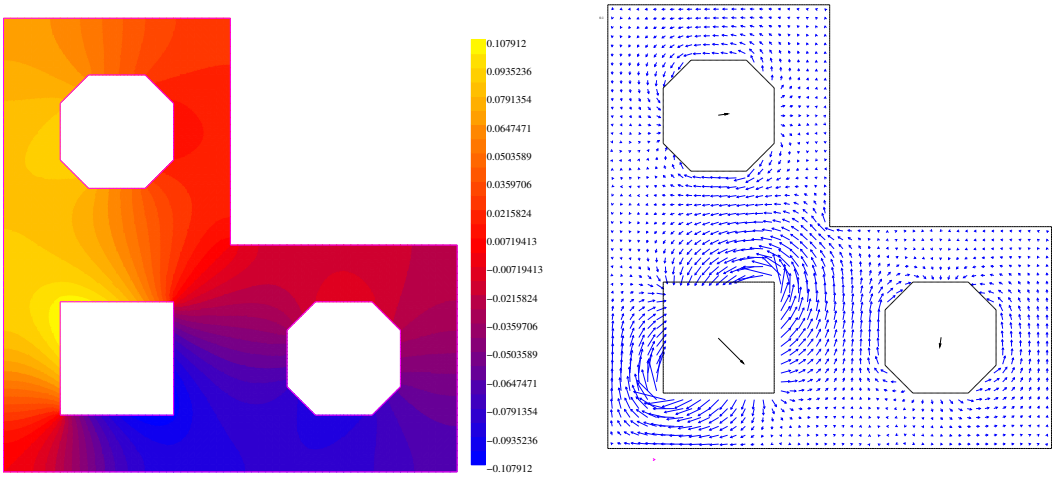

Figure 7. Test 1. Pressure field (left) and fluid velocity field (right)

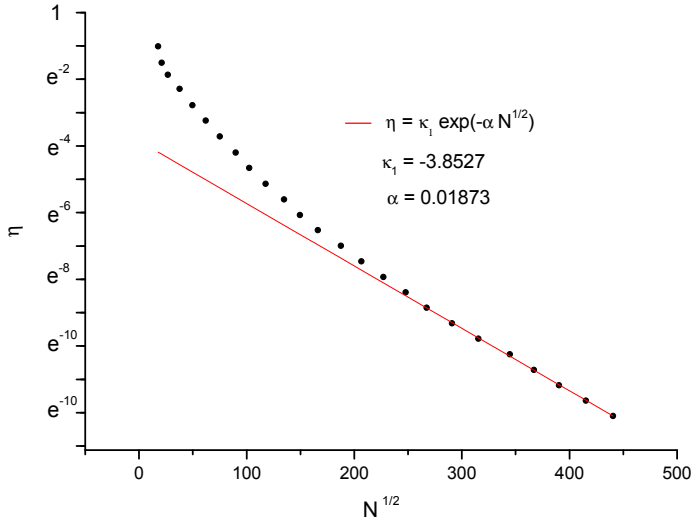

Figure 8. Test 1. η (logarithmic scale) versus $\sqrt{N}$

geometry, but also on the physical parameters of the tubes. Numerical evidence of the theoretically expected exponential convergence is also reported.

ACKNOWLEDGEMENTS

This work was partially supported by ANPCyT (Argentina) under grant PICT 2006-01307. The first author was partially supported by ANPCyT (Argentina) under grant PICT-2007-00910 and

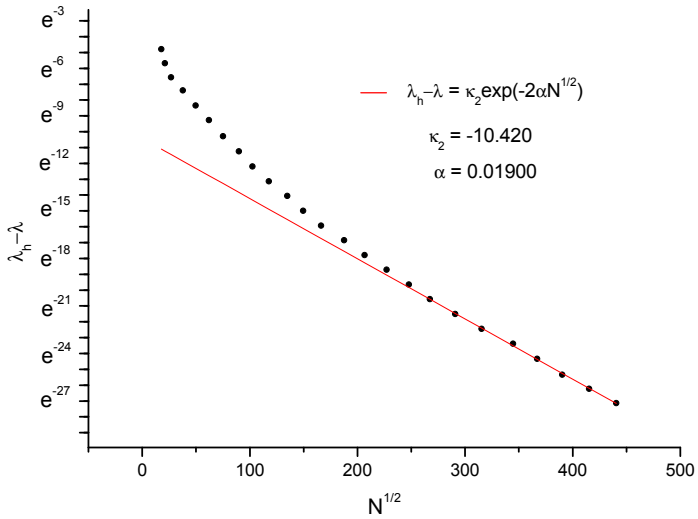

Figure 9. Test 1. $|\lambda_h - \lambda|$ (logarithmic scale) versus $\sqrt{N}$

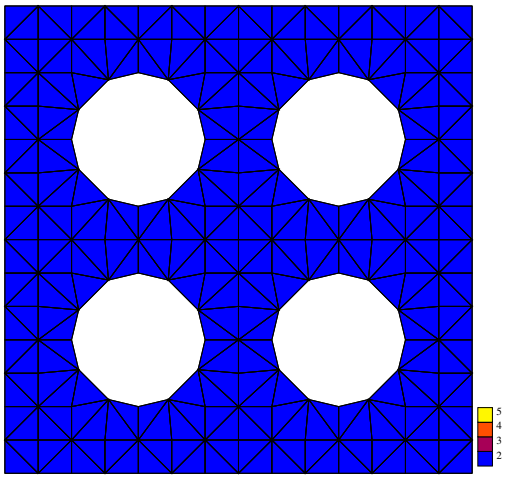

Figure 10. Test 2. Domain and initial mesh of the square cavity with four tubes.

by Universidad de Buenos Aires (Argentina) under grant X007. The first and second authors are members of CONICET (Argentina). The third author was partially supported by FONDAP and BASAL projects, CMM, Universidad de Chile (Chile).

REFERENCES

Table II. Test 2. Angular vibration frequencies

Mode	ω
1	0.9619
2	0.9627
3	0.9653
4	0.9661
5	0.9895
6	0.9921
7	0.9930
8	1.0026

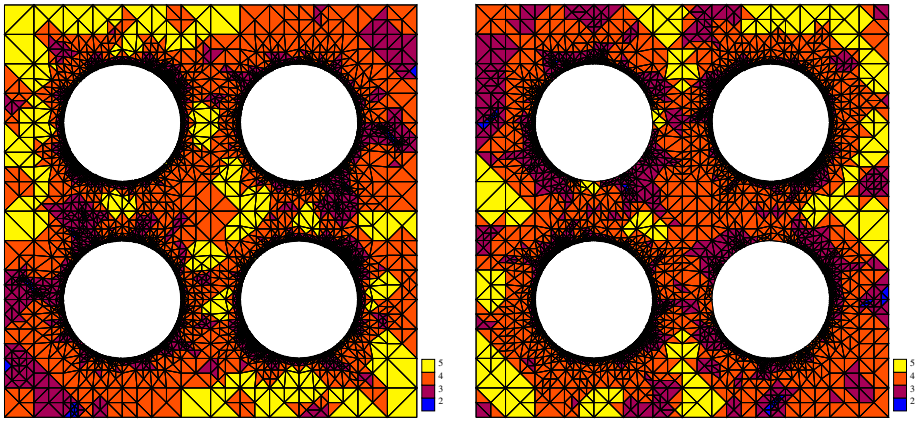

Figure 11. Test 2. Refined meshes at step 8: first mode (left) and sixth mode (right)

1. Armentano MG. The effect of reduced integration in the Steklov eigenvalue problem. *ESAIM: Mathematical Modelling and Numerical Analysis (M^2AN)* 2004; **38**(1):27–36.
2. Armentano MG, Padra C. A posteriori error estimates for the Steklov eigenvalue problem. *Applied Numerical Matematics* 2008; **58**:593–601.
3. Armentano MG, Padra C, Rodríguez R, Scheble M. An *hp* finite element adaptive scheme to solve the Laplace model for fluid-solid vibrations. Preprint DIM 2009-19, Universidad de Concepción, Concepción, 2009 (submitted).
4. Azaiez M, Deville MO, Gruber R, Mund EH. A new *hp* method for the −grad(div) operator in non-Cartesian geometries. *Applied Numerical Mathematics* 2008; **58**:985–998.
5. Bermúdez A, Durán R, Rodríguez R. Finite element solution of incompressible fluid-structure vibration problems. *International Journal for Numerical Methods in Engineering* 1997; **40**:1435–1448.
6. Bermúdez A, Rodríguez R, Santamarina D. A finite element solution of an added mass formulation for coupled fluid-solid vibrations. *Numerische Mathematik* 2000; **87**:201–227.
7. Boffi D. Approximation of eigenvalues in mixed form, discrete compactness property, and application to *hp* mixed finite elements. *Computer Methods in Applied Mechanics and Engineering* 2007; **196**:3672–368.
8. Boffi D, Costabel M, Dauge M, Demkowicz L. Discrete compactness for the *hp* version of rectangular edge finite elements. *SIAM Journal on Numerical Analysis* 2006, **44**:979–1004.
9. Conca C, Osses A, Planchard J. Asymptotic analysis relating spectral models in fluid-solid vibrations. *SIAM Journal on Numerical Analysis* 1998; **35**(3):1020–1048.

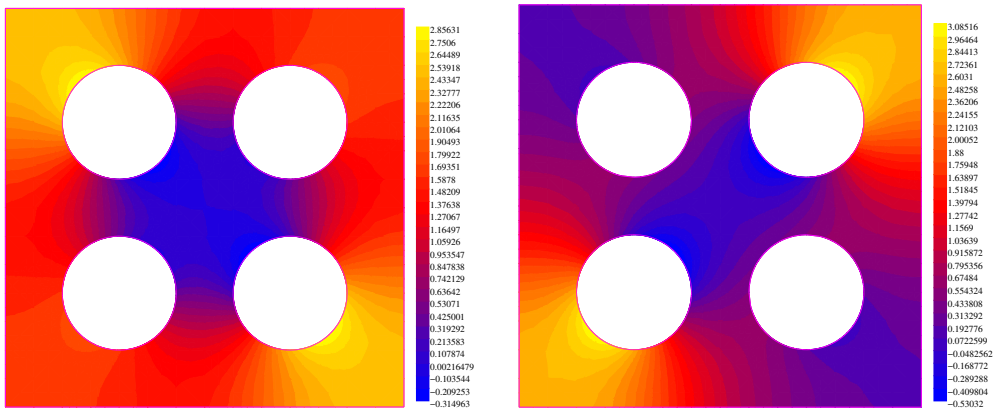

Figure 12. Test 2. Pressure field for the first mode (left) and the sixth mode (right)

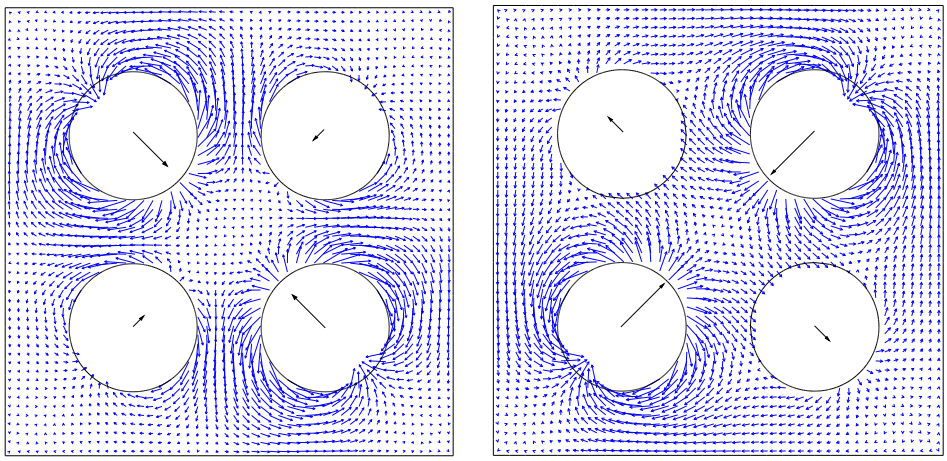

Figure 13. Test 2. Fluid velocity field for the first mode (left) and the sixth mode (right)

10. Conca C, Planchard J, Vanninathan M. *Fluid and Periodic Structures*, Wiley: Chichester, 1995.
11. Durán RG, Padra C, Rodríguez R. A posteriori error estimates for the finite element approximation of eigenvalue problems. *Mathematical Models and Methods in Applied Sciences (M3AS)* 2003; **13**:1219–1229.
12. Durán RG, Gastaldi L, Padra C. A posteriori error estimators for mixed approximations of eigenvalue problems. *Mathematical Models and Methods in Applied Sciences (M3AS)* 1999; **9**:1165–1178.
13. Larson MG. A posteriori and a priori error analysis for finite element approximations of self-adjoint elliptic eigenvalue problems. *SIAM Journal on Numerical Analysis* 2000; **38**:608–625.
14. Lovadina C, Lyly M, Stenberg R. A posteriori estimates for the Stokes eigenvalue problem. *Numerical Methods for Partial Differential Equations* 2009; **25**:244–257.
15. Melenk JM and Wohlmuth BI. On residual-based a posteriori error estimation in *hp*-FEM. *Advances in Computational Mathematics* 2001; **15**:311–331.
16. Morand HJP, Ohayon R. *Fluid-Structure Interaction*. Wiley: Chichester, 1995.
17. Planchard J. Eigenfrequencies of a tube bundle placed in a confined fluid. *Computer Methods in Applied Mechanics and Engineering* 1983; **30**:75–93.
18. Planchard J, Ibnou Zahir M. Natural frequencies of tube bundle in an uncompressible fluid. *Computer*

Methods in Applied Mechanics and Engineering 1983; **41**:47–68.
19. Verfürth R. *A review of a posteriori error estimation and adaptive mesh-refinement techniques*. Wiley & Teubner, 1996.

Centro de Investigación en Ingeniería Matemática (CI^{2}MA)

PRE-PUBLICACIONES 2009 - 2010

2009-17 Iuliu S. Pop, Florin A. Radu, Mauricio Sepúlveda, Octavio Vera: *Error estimates for the finite volume discretization for the porous medium equation*

2009-18 Raimund Bürger, Kenneth H. KARLSEN, Hector Torres, John D. Towers: *Second-order schemes for conservation laws with discontinuous flux modelling clarifier-thickener units*

2009-19 Maria G. Armentano, Claudio Padra, Rodolfo Rodríguez, Mario Scheble: *An hp finite element adaptive scheme to solve the Laplace model for fluid-solid vibrations*

2009-21 Carlos D. Acosta, Raimund Bürger, Carlos E. Mejia: *Monotone difference schemes stabilized by discrete mollification for strongly degenerate parabolic equations*

2009-22 Gabriel N. Gatica, Salim Meddahi: *Finite element analysis of a time harmonic Maxwell problem with an impedance boundary condition*

2009-23 Veronica Anaya, Mostafa Bendahmane, Mauricio Sepúlveda: *Mathematical and numerical analysis for predator-prey system in a polluted environment*

2009-24 Julio Aracena, Eric Fanchon, Marco Montalva, Mathilde Noual: *Combinatorics on update digraphs of discrete networks*

2010-01 Stefan Berres, Raimund Bürger, Rodrigo Garces: *Centrifugal settling of flocculated suspensions: A sensitivity analysis of parametric model functions*

2010-02 Mauricio Sepúlveda: *Stabilization of a second order scheme for a GKdV-4 equation modelling surface water waves*

2010-03 Lourenco Beirao-Da-Veiga, David Mora: *A mimetic discretization of the Reissner-Mindlin plate bending problem*

2010-04 Alfredo Bermúdez, Carlos Reales, Rodolfo Rodríguez, Pilar Salgado: *Mathematical and numerical analysis of a transient eddy current axisymmetric problem involving velocity terms*

2010-05 Maria G. Armentano, Claudio Padra, Rodolfo Rodríguez, Mario Scheble: *An hp finite element adaptive method to compute the vibration modes of a fluid-solid coupled system*

Para obtener copias de las Pre-Publicaciones, escribir o llamar a: Director, Centro de Investigación en Ingeniería Matemática, Universidad de Concepción, Casilla 160-C, Concepción, Chile, Tel.: 41-2661324, o bien, visitar la página web del centro: `http://www.ci2ma.udec.cl`







Centro de Investigación en
Ingeniería Matemática (CI²MA)
Universidad de Concepción

Casilla 160-C, Concepción, Chile
Tel.: 56-41-2661324/2661554/2661316
http://www.ci2ma.udec.cl